The Insertional Footprint of the Rotator Cuff: An Anatomic Study

Alan S. Curtis, M.D., Kelton M. Burbank, M.D., John J. Tierney, D.O., Arnold D. Scheller, M.D., and Andrew R. Curran, D.O.

Purpose: The purpose of this study was to define the entire rotator cuff footprint and relate it to known, easily identifiable landmarks as a guide for both open and arthroscopic rotator cuff repair. Anatomic: Gross and microscopic. **Methods:** The myotendinous units of the rotator cuff and their insertions onto the humerus were dissected in 20 fresh-frozen cadavers. The separate tendon insertions were identified, and their length and width measured. The character and exact anatomy of the tendons were also noted. The entire insertion was measured and referenced to the articular surface, biceps groove, and bare area of the humerus. In a separate part of the study, 6 cadavers were decalcified and thin-sliced through the supraspinatus tendon insertion. This insertion was evaluated via scanning electron microscopy (SEM). **Results:** Our findings demonstrated a consistent pattern at the insertion of the rotator cuff. The horseshoe-shaped insertion tapers away from the articular surface in a superior-to-inferior direction. Interdigitation of the muscle units may be noted, particularly between the supraspinatus and the infraspinatus. Average maximum insertional lengths and widths were as follows: subscapularis (SC): 40 × 20 mm; infraspinatus (IS): 29 × 19 mm; supraspinatus (SS): 23 × 16 mm; and teres minor (TM): 29 × 21 mm. The SC inserted on the lesser tuberosity adjacent to the biceps groove at the edge of the articular surface. It tapered away 18 mm at its inferior border. The SS inserted at the articular surface along its entire insertion from the bicipital groove to the top of the bare area. The IS wrapped the posterior border of the SS superiorly at the articular surface and tapered away inferiorly, framing the bare area. SEM microscopy showed the SS to be adherent to the edge of the articular surface medially. As it filled the sulcus, its lateral edge extended over the edge of the greater tuberosity. **Conclusions:** A consistent pattern was noted at the insertional anatomy of the rotator cuff. This anatomy was related to known, easily identifiable landmarks and may serve as a guide for evaluation of size, location, and propagation patterns of rotator cuff tears, as well as for their repair. **Clinical Relevance:** Knowledge of the insertional anatomy of the rotator cuff can facilitate grading and repair of rotator cuff tears. **Key Words:** Shoulder—Footprint—Rotator cuff—Rotator cuff tear—Partial rotator cuff tear

Rotator cuff tears may occur in a variety of patterns, ranging from small, partial-thickness, single-tendon tears to massive, full-thickness, multiple-tendon tears. Although the reported incidence of satisfactory results after repair is between 85% and 95%,[1] clearly not all rotator cuff tears are alike. Many factors can affect rotator cuff repair outcomes, including chronicity, location, size, and tissue quality.[1] However, an understanding of the normal anatomy of the rotator cuff, especially its attachment to the proximal humerus, is crucial to proper diagnosis and treatment of each tear type and is perhaps the single variable that is within the control of the shoulder surgeon. Use of this information allows restoration of the tendon or tendons to their proper anatomic positions, thus maximizing potential outcomes.

Despite its importance, relatively little has been written on the insertional anatomy of the rotator cuff. Clark and Harryman[2] were the first to meticulously review the

From the Division of Sports Medicine, New England Baptist Hospital (A.S.C., J.J.T., A.D.S.), Boston; Longview Orthopaedic Center (K.M.B.), Leominster, Massachusetts; and Saltzer Medical Group (A.R.C.), Nampa, Idaho, U.S.A.

Address correspondence and reprint requests to Alan S. Curtis, M.D., Boston Sports and Shoulder, 830 Boylston St, Chestnut Hill, MA 02467, U.S.A. E-mail: bsscurtis@aol.com

0749-8063/06/2206-0576$32.00/0

doi:10.1016/j.arthro.2006.04.001

Note: To access the supplementary tables accompanying this report, visit the June issue of *Arthroscopy* at www.arthroscopyjournal.org

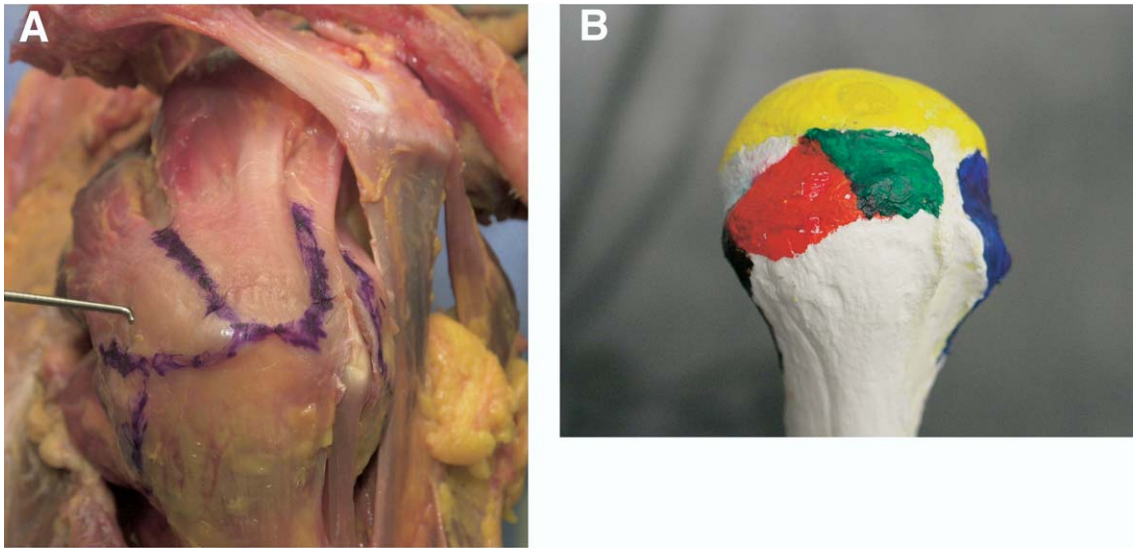

Figure 1. (A) Lateral view of intact myotendinous units with intervals marked prior to dissection. (B) Model showing footprints of the supraspinatus (green) and infraspinatus (red). The subscapularis footprint (blue) is anterior to the biceps groove.

character, thickness, and microscopic structure of the rotator cuff. Their study delineated 5 distinct layers with a combined average thickness of 9 to 12 mm. They also demonstrated that the supraspinatus (SS) and infraspinatus (IS) fibers fuse together laterally and are often difficult to separate from one another. Clark and Harryman, however, did not specifically outline the insertion onto the humerus. Minagawa et al.[3] were the first to delineate the insertions of the SS and IS and reference them to facets of the greater tuberosity.

In 1999, we first reported on the insertional anatomy of the rotator cuff.[4] Our findings demonstrated a consistent, measurable pattern that we called the *footprint*. Since then, others[5,6] have used this term as the concept and its applications have grown. The purpose of this article is to report in detail our original findings from the gross study of the footprint of each rotator cuff tendon and to add additional observations gained from study of the SS footprint with scanning electron microscopy (SEM). We define here the dimensions of the footprint for each rotator cuff tendon and relate these dimensions to known, easily identifiable landmarks to provide a guide for open and arthroscopic evaluation and treatment of patients with rotator cuff disease.

METHODS

Thirty-six fresh-frozen unpaired cadaver shoulders were evaluated in this study. The age and sex of the specimens were unknown. The cadavers were thawed at room temperature for 24 hours before undergoing dissection. Any tearing of the rotator cuff or osteophytic changes near the biceps groove, tuberosities, or bare area that would make measurement of the insertion inaccurate resulted in exclusion of a specimen from the study. Ten shoulders were eliminated in this manner.

Gross Dissection

Specimens consisted of the entire scapula, adjacent chest wall, and proximal one third of the humerus en bloc to ensure that each contained an intact glenohumeral joint. Twenty specimens were mounted in a vice, and superficial tissue was dissected off the underlying rotator cuff musculature. The proximal humerus and intact myotendinous units of the rotator cuff were thus isolated (Fig 1). Starting medially, we dissected along 3 intervals to isolate the individual tendon insertions—the rotator interval between the subscapularis (SC) and the SS, the interval between the SS and the IS, and the interval between the IS and the teres minor (TM). The tendons of the rotator cuff, especially the SS and IS, fuse together laterally and therefore are difficult to separate from one another in this area of tissue overlap. An incision was made in the central portion of each insertion, parallel with the fibers of the tendon, extending from the articular surface to the most lateral insertion on the tuberosity (Fig 2). This insertion was then dissected anteriorly and

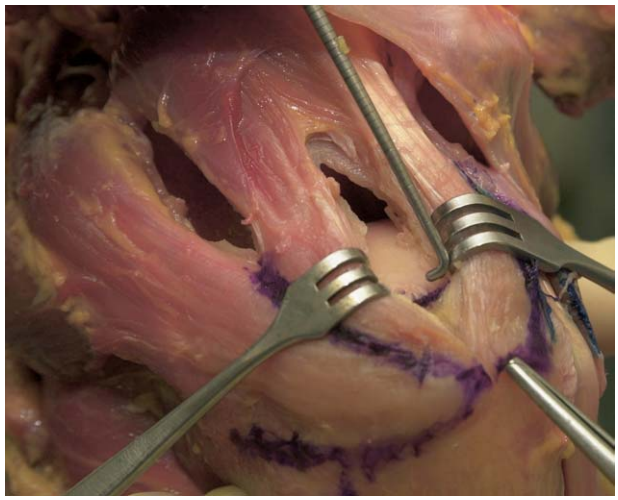

FIGURE 2. Dissection into the central portion of the supraspinatus tendon revealing its broad footprint.

posteriorly from the central incision. The separate tendons were then dissected free from their respective insertions on the humerus. Care was taken to mark the entire insertion. Shape, maximum length (anterior to posterior), and maximum width (medial to lateral) were measured and recorded for each tendon on every specimen. The delineated insertion was also measured and referenced from the articular surface, biceps groove, and bare area of the humerus.

Microscopy

In the second part of the study, 6 additional specimens were decalcified and then bisected through the midpoint of the SS footprint from medial to lateral, so that the microscopic characteristics of the insertion could be further evaluated. These specimens were fixed for 24 hours in 2.5% glutaraldehyde with cacodylic buffer. They were then dehydrated with alcohol before being critical-point-dried. Finally, they were coated with gold before they were viewed by means of SEM. They were then studied, with particular attention paid to the relationship of the insertion to the articular surface and the tuberosity.

RESULTS

Gross Findings

With use of the articular surface, biceps groove, and bare area as reference points, a consistent pattern of rotator cuff attachment was identified for each tendon.

Findings in the Subscapularis

The SC was the largest muscle–tendon unit. It inserted in a comma-shaped pattern (Fig 3) from 7 to 11 o'clock around the tuberosity (with the right shoulder used as a point of reference). The average maximum length was 40 mm (range: 35 to 55 mm), and the average maximum width was 20 mm (range: 15 to 25 mm) (Table 1, online only, available at www.arthroscopyjournal.org). It inserted along the medial aspect of the biceps groove, and its distance from the articular surface tapered from 0 mm superiorly to 18 mm inferiorly. The most superior intra-articular margin was purely tendinous. As the SC insertion ran inferiorly, it tapered to end as a purely musculocapsular attachment.

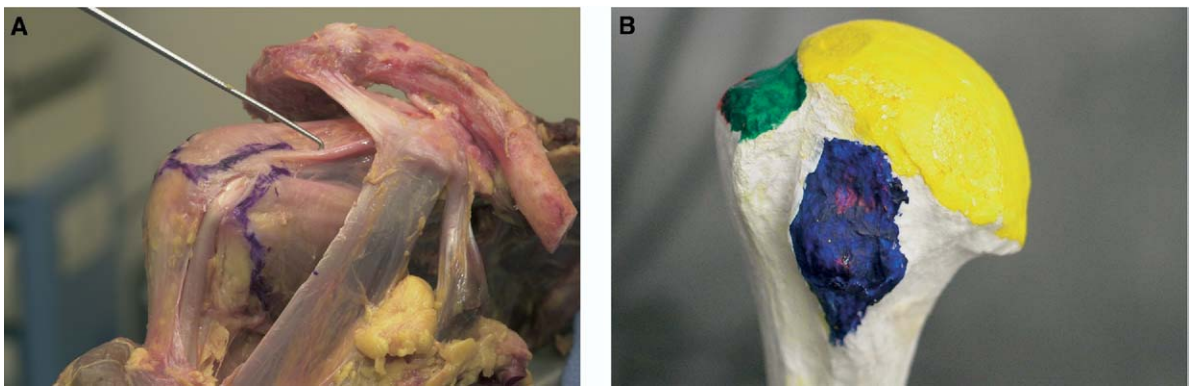

FIGURE 3. (A) Anterior view of the subscapularis on a cadaver before the footprint was dissected. (B) Footprint of the subscapularis (blue) on the model.

Findings in the Infraspinatus

The infraspinatus was second in size, inserting from approximately 1 to 3 o'clock. Superiorly, the IS interdigitated and wrapped around the posterior aspect of the SS tendon. The bipennate muscle tapered into a trapezoidal footprint (Fig 4) with an average maximum length of 29 mm (range: 20 to 45 mm) and width of 19 mm (range: 12 to 27 mm) (Table 2, online only, available at www.arthroscopyjournal.org). The insertion tapered away from the articular surface, from 0 mm superiorly to 16 mm inferiorly. The gap between the articular surface and the inferior insertion formed the "bare area." The tendon of the IS shortened and became more muscular as it ran toward the TM.

Findings in the Supraspinatus

The supraspinatus tendon was third in size. Its footprint filled the sulcus between the biceps groove and the bare area in a trapezoidal shape that was wider proximally along the articular surface compared with the more distal insertion around the tuberosity (Fig 5). The insertion was located from 11 to 1 o'clock. It had an average maximum length of 23 mm (range: 18 to 33 mm) and an average maximum width of 16 mm (range: 12 to 21 mm) (Table 3, online only, available at www.arthroscopyjournal.org). The insertion appeared at an average of 0.9 mm (range: 0 to 4 mm) from the edge of the articular surface, with most specimens having the SS insertion directly on the articular surface throughout the entire length of the tendon. The lateral most attachment actually continued over the lip of the greater tuberosity. The posterior border of the insertion was overlapped by the anterior border of the IS tendon. Although it was difficult to distinguish the beginning of one and the end of the other, the SS tended to insert closer to the articular surface.

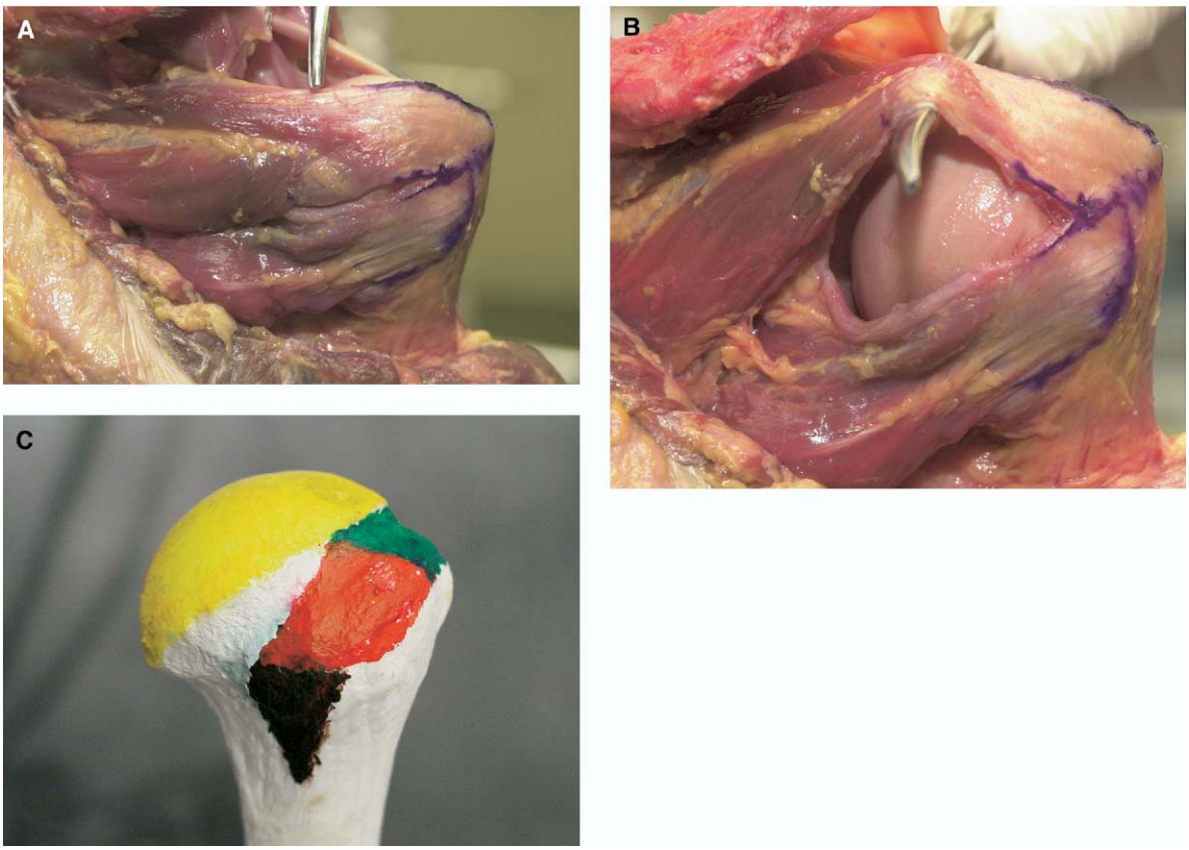

FIGURE 4. (A) Posterior view of a cadaver showing infraspinatus and teres minor. (B) Dissected interval between infraspinatus and teres minor. (C) Model showing footprints of infraspinatus (red) and teres minor (black), as well as supraspinatus (green).

Findings in the Teres Minor

The TM, the smallest muscle–tendon unit, had a relatively large footprint, inserting from 3 to 5 o'clock in a triangular shape (Fig 4). The average maximum length was 29 mm (range: 20 to 40 mm) and average width was 21 mm (range: 10 to 33 mm) (Table 4, online only, available at www.arthroscopyjournal.org). The insertion tapered rapidly from a few tendinous fibers superiorly, to purely muscle and capsule along the inferior half. Distance from the articular surface averaged 10 mm (range: 7 to 20 mm).

Microscopic Findings

SEM microscopy revealed that the SS tendon was densely adherent to the capsule. It then inserted onto the very edge of the articular surface. The insertion displayed an entirely tendinous, layered appearance that extended just over the lip of the greater tuberosity (Fig 6). The collagen microstructure was layered and well organized. However, as the tendon inserted onto the broad footprint, the actual width of each layer could not be reliably determined. The layers did, however, remain parallel in this transition zone.

DISCUSSION

In this study, we were able to show that each rotator cuff tendon has its own, unique, measurable insertion onto the humerus, which creates a footprint (Figs 1B, 3B, and 4C). We were able to obtain an average maximum length (in the anterior-posterior plane) and width (in the medial-lateral plane) for all 4 tendons. These dimensions were referenced to landmarks that are easily identifiable during both arthroscopic and open surgery: the biceps groove, the articular surface, and the bare area. On gross and microscopic analyses, the SS tendon inserted immediately adjacent to the articular margin; the IS and TM tapered laterally away from the margin to create the bare area. This knowledge of the footprint is important to the shoulder surgeon in several different ways. First, it is critical in the restoration of torn tendons back to their proper locations—a task made more difficult in chronic, neglected tears, wherein anatomic relationships may not be as obvious as in acute tears with minimal retraction. Assessment of the length and location of a tear relative to known landmarks and intervals can be used to enhance recognition of patterns of tears, as well as identification of which tendons are involved,[3] thus facilitating this difficult task (Fig 5B). In addition, because of its unique insertion immediately adjacent to the articular surface, one can use measurement of the width of a partial-thickness rotator cuff tear (PRCT) of the SS tendon, rather than depth, to obtain important information regarding the amount of tendon damage that has occurred and the need for treatment.[4,6] Finally, knowledge of the broad footprint has even led to changes in the techniques of repair, as evidenced by the increasing interest in dual or "double row" repair, which increases the surface area available for healing.[7,8]

At the time of our first report,[4] Clark and Harryman[2] had performed the only in-depth analysis of the

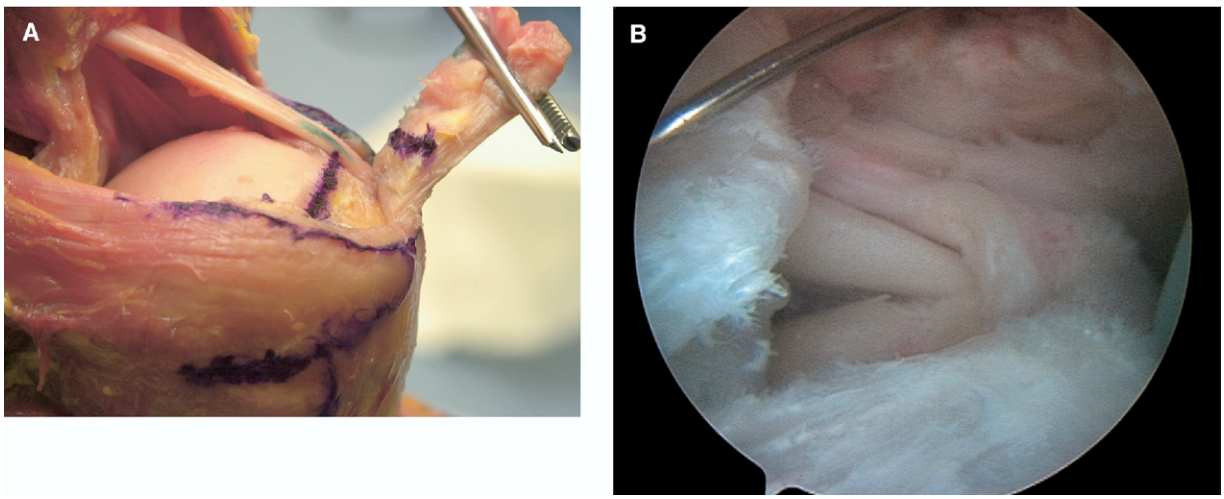

FIGURE 5. (A) Footprint of supraspinatus on cadaver. (B) Arthroscopic picture of a complete supraspinatus tendon tear along rotator interval anteriorly and infraspinatus/supraspinatus interval posteriorly, exposing the footprint. This is a "tongue"-type tear.

entire rotator cuff insertion. Although their gross and microscopic work elegantly demonstrated a distinct 5-layer pattern with significant blending of fibers, they did not measure any dimension of the insertion other than thickness. Minagawa et al.[3] were the first to measure any tendon insertions, focusing on the length and overlap of the SS and IS tendons as a guide for surgical repair. They did not, however, measure the width of the insertions. Ellman[9] commented on the close proximity of the SS tendon to the articular surface. He proposed measuring the base (length) and width of both full- and partial-thickness tears to quantify an "area of defect." When developing his classification system for partial tears, however, he chose to use the depth of the tear, rather than relate it to the amount of exposed footprint. We then presented our original paper, outlining the footprint and its potential value, particularly in assessing PRCTs. Since then, others have expanded on these concepts. Ruotolo[6] used this idea to formally define a method of evaluating articular side partial-thickness RCTs. He measured the width of the tear, that is, the amount of the tendon that has avulsed off in the medial-to-lateral plane. Originally described as a "rim rent" by Codman,[10] this is the most common type of PRCT and likely is the origin of most full-thickness rotator cuff tears. Arthroscopic measurement of the amount of exposed footprint as a percentage of the total footprint is perhaps a more objective and efficient way of assessing these tears than is measuring the depth of the tear. In their own description of their technique, however, the term *depth* appears in place of *width*, leading to confusion. Nonetheless, we have been using a similar technique to assess PRCTs since our original report and have had good, reproducible success (Fig 7).

Dugas et al.[5] rejuvenated Ellman's idea of surface area—a concept with unknown relevance. They measured all 4 tendons, but their values were significantly lower than other published numbers.[3,4,6] It is well understood that the tendons do overlap near their insertion onto the humerus. This can make defining the interval difficult and somewhat arbitrary. We, however, noted a pattern whereby the SS fibers tended to insert closer to the articular surface, while the IS fibers intertwined and crossed over to insert more laterally and anteriorly on the tuberosity. This 5- to 10-mm overlap zone was located just anterior to the tip of the bare area, which is an arthroscopic landmark for the SS–IS interval. The IS footprint extended inferiorly on the greater tuberosity, essentially framing the upper half of the bare area. Perhaps this is why our results correlate better with other reports on the length of the SS footprint. It is interesting to note that our width average was slightly greater on average because of our noting that the fibers of the SS insertion fill the sulcus from the articular surface to the tuberosity and actually extend slightly beyond the tuberosity tip—a fact that we later confirmed via microscopy.

Our results also show that the SS footprint began immediately adjacent to the articular cartilage, a finding that has been replicated by other reports. This information is important for the assessment of PRCTs, as mentioned earlier, but also for the repair of full-thickness tears. The purely tendinous SS filled the sulcus from the articular cartilage to the tuberosity, averaging 16 mm in width. This indicates that any repair that does not impinge upon the articular surface or extend beyond the tuberosity is within the anatomic footprint. In a study by Lui et al.,[11] the biomechanical effect of rotator cuff repair location was evaluated. They concluded that the midpoint of the tendon insertion could be moved up to 10 mm medially with no resultant negative biomechanical consequences. Given the normal insertional anatomy, an ideal repair should re-create a wide zone of tendon–bone contact, which should enhance healing and theoretically dissipate forces over a greater area. This is the concept that has recently popularized the "double row" repair technique.

One of the weaknesses of this study is the lack of information regarding age, sex, and size of the cadavers. It is likely that sex, height, and perhaps weight would independently influence the size of the rotator cuff footprints. It is unclear what effect age might

Figure 6. SEM of supraspinatus footprint.

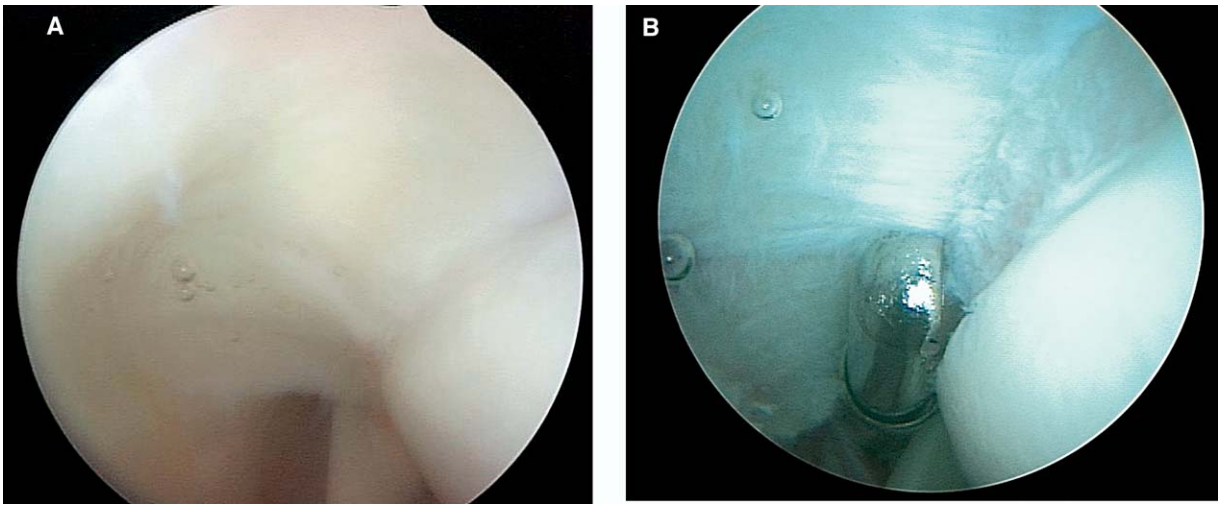

FIGURE 7. (A) Normal insertion of supraspinatus along articular margin as seen through arthroscope. (B) Partial-thickness tear of supraspinatus with exposed footprint along the articular margin.

have on the footprint. Future studies might look at these relationships.

CONCLUSIONS

A consistent pattern of attachment of rotator cuff tendons to the humerus was delineated. We have called this insertional anatomy the *footprint*. The horseshoe-shaped pattern tapers away from the articular surface from superior to inferior. The character of the insertion also tapers, from pure tendon superiorly to muscle and capsule inferiorly. The insertion is quite broad with significant interdigitation between muscle–tendon units. An understanding of the footprint may allow the arthroscopist to grade PRCTs from the articular side and may guide both the arthroscopist and the open surgeon to restore torn tendons to their functional anatomic positions.

Acknowledgement: The authors would like to acknowledge the efforts of Dr. E. J. Hayek and Karen Hodgens in providing assistance with electron microscopy.

REFERENCES

1. Ianotti JP. Full-thickness rotator cuff tears: Factors affecting surgical outcome. *J Am Acad Orthop Surg* 1994;2:87-95.
2. Clark JM, Harryman DT II. Tendons, ligaments, and capsule of the rotator cuff: Gross and microscopic anatomy. *J Bone Joint Surg Am* 1992;74:713-725.
3. Minagawa H, Itoi E, Konno N, et al. Humeral attachment of the supraspinatus and infraspinatus tendons: An anatomic study. *Arthroscopy* 1998;14:302-306.
4. Tierney JJ, Curtis AS, Kowalik DL, Scheller AD. The footprint of the rotator cuff. *Arthroscopy* 1999;15:556-557.
5. Dugas JR, Campbell DA, Warren RF, Robie BH, Millett PJ. Anatomy and dimensions of rotator cuff insertions. *J Shoulder Elbow Surg* 2002;11:498-503.
6. Ruotolo C, Fow JE, Nottage WM. The supraspinatus footprint: An anatomic study of the supraspinatus insertion. *Arthroscopy* 2004;20:246-249.
7. Lo IK, Burkhart SS. Double-row arthroscopic rotator cuff repair: Re-establishing the footprint of the rotator cuff. *Arthroscopy* 2003;19:1035-1042.
8. Millett PJ, Mazzocca A, Guanche CA. Mattress double anchor footprint repair: A novel, arthroscopic rotator cuff repair technique. *Arthroscopy* 2004;20:875-879.
9. Ellman H. Diagnosis and treatment of incomplete rotator cuff tears. *Clin Orthop* 1990;254:64-74.
10. Codman EA. *The shoulder.* Boston: Thomas Todd, 1934.
11. Lui J, Hughes RE, O'Driscoll SW, An K. Biomechanical effect of medial advancement of supraspinatus tendon. *J Bone Joint Surg Am* 1998;80:853-859.

TABLE 1. *Subscapularis*

Spec #	Length	Width	Side
1	55 mm	20 mm	R
2	35 mm	18 mm	R
3	36 mm	16 mm	R
4	35 mm	20 mm	L
5	50 mm	20 mm	R
6	40 mm	20 mm	R
7	40 mm	19 mm	R
8	35 mm	19 mm	L
9	36 mm	16 mm	L
10	35 mm	18 mm	R
11	30 mm	15 mm	R
12	30 mm	25 mm	R
13	40 mm	25 mm	R
14	40 mm	25 mm	L
15	45 mm	25 mm	R
16	45 mm	15 mm	L
17	46 mm	18 mm	L
18	45 mm	20 mm	L
19	44 mm	18 mm	R
20	45 mm	20 mm	L
Average:	**40 mm**	**20 mm**	
Range:	**35-55 mm**	**15-25 mm**	

TABLE 2. *Infraspinatus*

Spec #	Length	Width	Side
1	30 mm	20 mm	R
2	20 mm	18 mm	R
3	28 mm	18 mm	R
4	25 mm	15 mm	L
5	25 mm	23 mm	R
6	30 mm	15 mm	R
7	25 mm	19 mm	R
8	30 mm	18 mm	L
9	20 mm	18 mm	L
10	30 mm	20 mm	R
11	38 mm	12 mm	R
12	28 mm	17 mm	R
13	45 mm	27 mm	R
14	25 mm	18 mm	L
15	22 mm	20 mm	R
16	28 mm	20 mm	L
17	27 mm	22 mm	L
18	32 mm	24 mm	L
19	23 mm	17 mm	R
20	40 mm	12 mm	L
Average:	**29 mm**	**19 mm**	
Range:	**20-45 mm**	**12-27 mm**	

TABLE 3. *Supraspinatus*

Spec #	Length	Width	Side
	23 mm	16 mm	R
2	20 mm	14 mm	R
3	20 mm	18 mm	R
4	18 mm	15 mm	L
5	25 mm	20 mm	R
6	20 mm	15 mm	R
7	22 mm	20 mm	R
8	27 mm	16 mm	L
9	33 mm	17 mm	L
10	18 mm	12 mm	R
11	33 mm	21 mm	R
12	20 mm	12 mm	R
13	22 mm	17 mm	R
14	30 mm	15 mm	L
15	25 mm	20 mm	R
16	25 mm	15 mm	L
17	25 mm	17 mm	L
18	25 mm	17 mm	L
19	23 mm	16 mm	R
20	21 mm	18 mm	L
Average:	**23 mm**	**16 mm**	
Range:	**18-33 mm**	**12-21 mm**	

TABLE 4. *Teres Minor*

Spec #	Length	Width	Side
1	35 mm	33 mm	R
2	25 mm	25 mm	R
3	35 mm	23 mm	R
4	40 mm	25 mm	L
5	25 mm	23 mm	R
6	35 mm	23 mm	R
7	25 mm	23 mm	R
8	35 mm	23 mm	L
9	25 mm	25 mm	L
10	20 mm	10 mm	R
11	20 mm	10 mm	R
12	27 mm	14 mm	R
13	20 mm	10 mm	R
14	22 mm	12 mm	L
15	34 mm	20 mm	R
16	35 mm	24 mm	L
17	39 mm	25 mm	L
18	27 mm	23 mm	L
19	28 mm	20 mm	R
20	28 mm	20 mm	L
Average:	**29 mm**	**21 mm**	
Range:	**20-40 mm**	**10-33 mm**	